

## Novel Rhenium Nitrides

Alexandra Friedrich,<sup>1,\*</sup> Björn Winkler,<sup>1</sup> Lkhamsuren Bayarjargal,<sup>1</sup> Wolfgang Morgenroth,<sup>1</sup> Erick A. Juarez-Arellano,<sup>2</sup> Victor Milman,<sup>3</sup> Keith Refson,<sup>4</sup> Martin Kunz,<sup>5</sup> and Kai Chen<sup>5</sup>

<sup>1</sup>*Geowissenschaften, Goethe-Universität, Altenhöferallee 1, D-60438 Frankfurt a. M., Germany*

<sup>2</sup>*Universidad del Papaloapan, Circuito Central 200, Parque Industrial, Tuxtpec 68301, México*

<sup>3</sup>*Accelrys, 334 Science Park, Cambridge CB4 0WN, United Kingdom*

<sup>4</sup>*Rutherford-Appleton Laboratory, Chilton, Didcot, Oxfordshire OX11 0QX, United Kingdom*

<sup>5</sup>*Advanced Light Source, Lawrence Berkeley National Laboratory, 1 Cyclotron Road, Berkeley, California 94720, USA*

(Received 28 May 2010; published 20 August 2010)

We report the synthesis, structure, and properties of novel bulk rhenium nitrides, hexagonal  $\text{Re}_2\text{N}$ , and  $\text{Re}_3\text{N}$ . Both phases have very high bulk moduli of  $>400$  GPa, similar to the most incompressible binary transition-metal (TM) carbides and nitrides found to date. However, in contrast to other incompressible TM carbides and nitrides,  $\text{Re}_3\text{N}$  is better placed for potential technological applications, as it can be formed at relatively moderate pressures (13–16 GPa) and temperatures (1600–2400 K).

DOI: 10.1103/PhysRevLett.105.085504

PACS numbers: 61.05.cp

It is well known that the introduction of smaller atoms such as nitrogen and carbon into interstitial sites in close-packed TM lattices leads to dramatic changes of the physical properties of the compound with respect to that of the metal, such as increasing melting temperatures to nearly 4000 K in some binary TM carbides. Numerous binary TM borides and carbides have found applications as abrasives or “ultra high-temperature ceramics” [1,2]. The origin of the unusual properties is the complex bonding found in these compounds, where there are metal-metal, metal-nonmetal and nonmetal-nonmetal contacts. The systematic search for further materials with outstanding mechanical properties such as a very high bulk modulus focuses on two main approaches: The combination of light elements like in the B/C/N/O system [3] or new nanocarbon systems [4,5] to form short covalent bonds, and the formation of compounds based on metals with high densities of valence electrons, such as rhenium, osmium, and iridium [3]. Novel nitrides and carbides formed with these metals would complement the extensive knowledge available for binary nitrides and carbides formed by transition metals of groups IV–VI (Hf, Ta, W) [6]. The known transition-metal nitrides and carbides of the remaining period 6 elements (Re, Os, Ir, Pt, Au, Hg) are orthorhombic  $\text{OsN}_2$  [7], trigonal  $\text{IrN}_2$  [7,8], cubic  $\text{PtN}_2$  [8,9], hexagonal  $\text{Re}_2\text{C}$  [10], and cubic  $\text{PtC}$  [11]. Rhenium nitrides  $\text{ReN}_x$ ,  $0.06 < x < 1.35$  have been reported from high-temperature synthesis using precursors [12–14] and from thin films [15–17]. However, the samples had small crystallite sizes, and fcc and hcp crystal structures were proposed. It was claimed that the direct synthesis of rhenium nitride from the elements is not possible at high temperature [12,13]. Up to now, there is no clear crystal chemical understanding on whether dinitrogen units would be incorporated (such as in  $\text{OsN}_2$ ,  $\text{IrN}_2$ , and  $\text{PtN}_2$ ), or whether the  $\text{N}_2$  dissociates. It is undisputed that nitrogen dissociates during the formation of, e.g.,  $\text{TaN}$ ,  $\text{TiN}$ , or  $\text{Ta}_2\text{N}_3$ . In this study, we present the synthesis of

two novel rhenium nitrides at high pressures and temperatures in the laser-heated diamond anvil cell and the sample characterization by white beam Laue microdiffraction and complementary density functional theory based calculations.

Small pieces of rhenium were cut from a rhenium foil ( $>99.98\%$ ) and loaded into holes of 120–160  $\mu\text{m}$  diameter in tungsten gaskets preindented to thicknesses of 38–46  $\mu\text{m}$  in Boehler-Almax diamond anvil cells. For the thermal insulation single-crystalline sapphire chips of  $<5$   $\mu\text{m}$  thickness or compressed KCl were placed on top of both diamond anvils. Pressure was determined by the ruby fluorescence method [18]. Nitrogen was loaded within a pressure vessel as both a reaction compound and a pressure transmitting medium. Powder x-ray diffraction at high pressure and high temperature was performed at the Advanced Light Source (ALS, LBNL, Berkeley, beam line 12.2.2) using double-sided laser heating with two 100 W fiber lasers (1090 nm), 25 keV radiation, and a MAR345 image plate as detector [19]. Data collection was done with a  $10 \times 10$   $\mu\text{m}^2$  beam spot. The laser spots had a diameter of about 30  $\mu\text{m}$ . The diffraction data were processed using FIT2D [20], DATLAB [21], FULLPROF [22], TREOR [23], and GSAS [24]. *In situ* diffraction data were collected at pressures between ambient and 32 GPa during and without laser heating.

The synchrotron x-ray Laue microdiffraction experiment was carried out at beam line 12.3.2 of the ALS [25]. A polychromatic ( $5 \text{ keV} < E < 22 \text{ keV}$ ) x-ray beam was focused to  $\approx 1 \times 1$   $\mu\text{m}^2$  by a pair of Kirkpatrick-Baez mirrors. The diffraction experiment was conducted in reflection mode with the sample plane inclined by  $45^\circ$  to the incident beam and the CCD area detector (MAR133) at  $90^\circ$ . The Laue patterns were indexed using XMAS v.5 [26]. Monochromator scans on individual grains were performed by employing a 4-bounce Si(111) monochromator.

Density functional theory (DFT) calculations were performed using the CASTEP code [27]. The code is an implementation of Kohn-Sham DFT based on a plane wave basis set in conjunction with pseudopotentials. The plane wave cutoff was set to 600 eV. All pseudopotentials were ultrasoft and were generated using the Wu-Cohen generalized gradient approximation functional [28]. The rhenium pseudopotential is characterized by a core radius of 2.1 a.u. and the  $5s$  and  $5p$  semicore states were treated as valence states. The nitrogen pseudopotential had a core radius of 1.5 a.u. The Brillouin-zone integrals were performed using Monkhorst-Pack grids [29] with spacings between grid points of less than  $0.02 \text{ \AA}^{-1}$ . Full geometry optimizations at pressures between 0–50 GPa were performed so that forces were converged to  $0.004 \text{ eV/\AA}$  and the stress residual to 0.05–0.150 GPa. Elastic stiffness coefficients were obtained by the stress-strain method, and phonons were computed by the finite displacement technique for both phases. For thermodynamic comparisons, the reference state for carbon was diamond, while for nitrogen at ambient pressure, the energy of an  $\text{N}_2$  molecule in a  $15^3 \text{ \AA}^3$ -box was employed. At pressures above 7 GPa, the reference state for nitrogen was  $\epsilon$ -nitrogen.

Rhenium foil embedded in nitrogen remains stable during heating experiments at 10.0(5) GPa and temperatures up to 2800 K. A typical x-ray powder diffraction pattern measured at the ALS at 13.1(1) GPa before laser heating is shown in Fig. 1. This diffraction pattern can be completely indexed by assigning peaks to either rhenium,  $\delta\text{-N}_2$ , or tungsten. Weak diffraction lines from the tungsten gasket stem from the diffraction of weak tails of the  $10 \times 10 \mu\text{m}^2$  beam. When laser heating the rhenium foil embedded in nitrogen at 13(1) GPa and temperatures of 1700(200) K, a novel rhenium nitride (phase I) is formed (Fig. 1).

This phase is stable on successive laser heating up to 2250(150) K at pressures between 10.5–16 GPa. The reaction of the rhenium foil can easily be observed by the formation of spotty powder diffraction rings. Phase I can be fully indexed by a hexagonal cell in space group  $P\bar{6}m2$  (Table I). During laser heating at about 2000 K at pressures of 20(2) GPa, another novel rhenium nitride (phase II) is formed and becomes the stable phase. Phase II can be fully indexed by a hexagonal cell in space group  $P6_3/mmc$  (Fig. 1, Table I). Both phases can be recovered at ambient conditions.

Rietveld refinement showed that phase I has three Re atoms in the unit cell and an  $ABB$  stacking sequence. Phase II has a stacking sequence  $AABB$  with four Re atoms per unit cell, identical to that of  $\text{Re}_2\text{C}$  [10,30]. Because of the strong difference in the scattering cross section, the Rietveld refinement gave the positions of the rhenium atoms only. As in our earlier study on rhenium carbide, the positions of the nitrogen atoms were obtained by performing density functional theory calculations on a sequence of trial structures. A systematic and exhaustive test of all reasonable structures under the constraints of

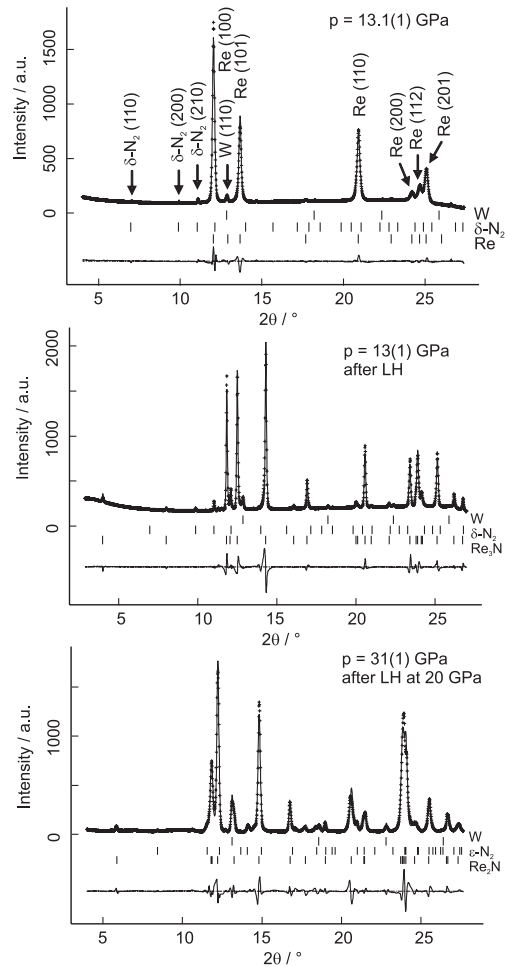


FIG. 1. Powder x-ray diffraction patterns ( $\lambda = 0.4958 \text{ \AA}$ ) showing, from top to bottom, unreacted rhenium foil at 13.1(1) GPa, the presence of  $\text{Re}_3\text{N}$  after laser heating at 1700 (200) K at 13(1) GPa, and the presence of  $\text{Re}_2\text{N}$  at 31(1) GPa after reaction during laser heating at 20(2) GPa and pressure increase. Symbols (+) represent experimental values. The result of the Le Bail fit is shown by the continuous line through the data points. Vertical bars show the positions of the allowed Bragg reflections of the different phases. The difference curve is plotted below each fit.

hexagonal cells with either three (stacking sequence  $ABB$ ) or four (stacking sequence  $AABB$ ) rhenium atoms in a unit cell with DFT models showed that the two sets of experimentally known lattice parameters could only successfully be reproduced by two models related to the  $\text{Re}_2\text{C}$  structure. Phase I corresponds to  $\text{Re}_3\text{N}$  [space group  $P\bar{6}m2$ , Re on Wyckoff positions  $1(f)$  and  $2(h)$  with  $z = 0.198$ , N on  $1(e)$ ], while phase II has the composition  $\text{Re}_2\text{N}$  [space group  $P6_3/mmc$ , Re on Wyckoff position  $4(f)$  with  $z = 0.106$  and N on  $2(d)$ ]. The crystal structures of Re,  $\text{Re}_3\text{N}$ , and  $\text{Re}_2\text{N}$  are shown in Fig. 2. While by this approach we can exclude that, for example, a nitrogen atom is located on Wyckoff position  $2(b)$  in  $\text{Re}_2\text{N}$  (which would be possible from packing considerations, but leads to a significantly extension of the  $c$ -lattice parameter), we cannot study site

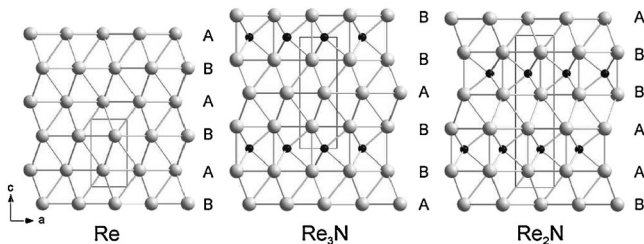
TABLE I. Selected refined and calculated cell parameters.  $\text{Re}_3\text{N}$  (phase I) crystallizes in space group  $P\bar{6}m2$ , Re, and  $\text{Re}_2\text{N}$  (phase II) have space group  $P6_3/mmc$ .

Phase	$a/\text{\AA}$	$c/\text{\AA}$	comment
Re	2.73107(8)	4.4100(9)	starting material at 13(1) GPa
Re	2.7251	4.4019	from DFT at 13 GPa
$\text{Re}_3\text{N}$	2.77759(7)	7.0972(5)	reaction product at 13(1) GPa after LH at $\approx 1700$ K
$\text{Re}_3\text{N}$	2.7764	7.0566	from DFT at 13 GPa
$\text{Re}_2\text{N}$	2.7767(1)	9.741(1)	reaction product at 20(2) GPa after LH at $>2000$ K
$\text{Re}_2\text{N}$	2.7856	9.6833	from DFT at 20 GPa
$\text{Re}_2\text{N}$	2.7692(2)	9.644(2)	reaction product at 31(1) GPa
$\text{Re}_2\text{N}$	2.7619	9.6436	from DFT at 31 GPa
$\text{Re}_3\text{N}$	2.8105(5)	7.154(2)	recovered, ambient conditions, powder diffraction
$\text{Re}_3\text{N}$	2.78(1)	7.152(4)	recovered, ambient conditions from single crystals
$\text{Re}_3\text{N}$	2.8065	7.112	from DFT at 0 GPa
$\text{Re}_2\text{N}$	2.8442(5)	9.796(2)	recovered, ambient conditions, powder diffraction
$\text{Re}_2\text{N}$	2.83(5)	9.88(1)	recovered, ambient conditions from single crystals
$\text{Re}_2\text{N}$	2.837	9.799	from DFT at 0 GPa

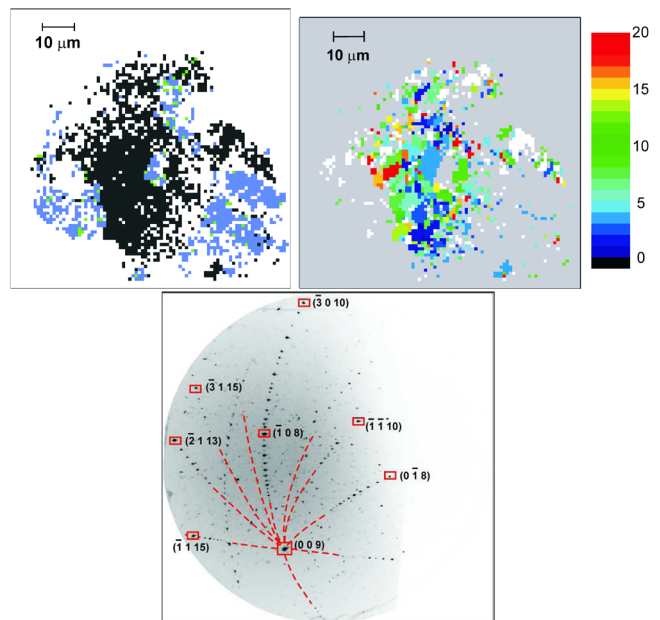
occupancies in detail. However, the overall agreement between observed and calculated structural parameters is so satisfactory that we conclude that the compounds are either stoichiometric or very nearly so.

White beam x-ray microdiffraction on recovered samples at the ALS was used to further characterize the reaction products. A representative map of a sample recovered from synthesis conditions favoring the formation of  $\text{Re}_3\text{N}$  is given in Fig. 3, where areas, in which  $\text{Re}_3\text{N}$  and Re were successfully indexed, are shown in black and gray (blue), respectively.

It can be seen that in the central part, the sample converted to  $\text{Re}_3\text{N}$ , whereas in the outside rim, where heating was less intense, Re remained unreacted. Maps of the grain orientations (Fig. 3) show the polycrystalline nature of the reaction product with individual grains between  $\approx 3 \mu\text{m}$  and  $\approx 8 \mu\text{m}$  in size. The quality of the indexing of a single grain is shown in Fig. 3. Monochromator scans on selected reflections [e.g., for  $\text{Re}_3\text{N}$  (0 0 9), (0 0 10), ( $\bar{1}$  0 8), ( $\bar{2}$  1 13)] allowed the determination of the cell parameters [ $\text{Re}_3\text{N}$ :  $a = 2.78(1) \text{\AA}$ ,  $c = 7.152(4) \text{\AA}$ ;  $\text{Re}_2\text{N}$ :  $a = 2.83(5) \text{\AA}$ ,  $c = 9.88(1) \text{\AA}$ ], consistent with the results of the x-ray powder diffraction. This unambiguously confirms the powder diffraction indexing and shows that the reaction products indeed are single phase  $\text{Re}_3\text{N}$  and  $\text{Re}_2\text{N}$ .

FIG. 2. Comparison between the crystal structures of Re,  $\text{Re}_3\text{N}$ , and  $\text{Re}_2\text{N}$ .

Structure-property relations were obtained both from experiment and the DFT model calculations. The computed bulk modulus is 413 and 415 GPa for  $\text{Re}_3\text{N}$  and  $\text{Re}_2\text{N}$ , respectively. This is in good agreement with the experimental data, where a fit with a 2nd order Birch Murnaghan equation of state gave a bulk

FIG. 3 (color online). Typical results from white beam x-ray microdiffraction showing a map of the phase distribution ( $\text{Re}_3\text{N}$  and Re in black and gray (blue) areas, respectively, top left), the distribution of the grains and their sizes ( $\approx 3\text{--}8 \mu\text{m}$ ) derived from the coherent regions of  $c$ -axis orientations relative to the sample normal of  $\text{Re}_3\text{N}$  (top right), and an image indexed with the unit cell of  $\text{Re}_3\text{N}$  (bottom). The indices of a few reflections are shown as examples. The dashed curves (red) indicate extensions of the indexed Laue zones.

modulus of  $B = 395(7)$  GPa for  $\text{Re}_3\text{N}$ , and  $B = 401(10)$  GPa for  $\text{Re}_2\text{N}$ . The DFT calculations showed that in the athermal limit,  $\text{Re}_2\text{N}$  and  $\text{Re}_3\text{N}$  are more stable by  $\approx 0.25$  eV/Re-atom than the mixture of the elements. The mechanical stability of  $\text{Re}_3\text{N}$  has also been demonstrated by phonon calculations, which showed no soft mode in the range of 0–20 GPa. A population analysis of the Re-N bonds shows that they are rather covalent, with a bond population of  $\approx 0.75 e^-/\text{\AA}^3$ .

In summary, we have synthesized and structurally characterized bulk rhenium nitrides for the first time, and, as was expected, they are very incompressible. In contrast to other transition-metal nitrides, the synthesis conditions for  $\text{Re}_3\text{N}$  can actually be achieved in large volume presses. There are close relationships between the group IV–VI carbides and the corresponding nitrides. Such a relationship has also now been established for Re compounds, as  $\text{Re}_2\text{C}$ ,  $\text{Re}_2\text{N}$ , and  $\text{Re}_3\text{N}$  are structurally related and in fact are all equally incompressible. From crystal chemical arguments, such as the similarity between the radii of C and N, the observation of these two new structures strengthens our prediction [30] that an osmium carbide phase will crystallize in this structure family, i.e., probably will have the same structure as either  $\text{Re}_3\text{N}$  or  $\text{Re}_2\text{N}$ .

Financial support from the DFG, Germany, within SPP1236 (Projects FR-2491, WI-1232), the BMBF, Germany (Project 05KS7RF1), the Vereinigung der Freunde und Förderer der Goethe-Universität, and the FOKUS program of the Goethe University is gratefully acknowledged. CASTEP calculations were performed on STFC E-Science facility. The Advanced Light Source is supported by the Director, Office of Science, Office of Basic Energy Science, of the U.S. Department of Energy under Contract No. DE-AC02-05CH11231. This research was partially supported by COMPRES under NSF Cooperative Agreement No. EAR 06-49658. We also thank S. M. Clark and J. Yan (ALS) for technical support at beam line 12.2.2.

\*friedrich@kristall.uni-frankfurt.de

- [1] E. Opila, S. Levine, and J. Lorincz, *J. Mater. Sci.* **39**, 5969 (2004).
- [2] Y. D. Blum, J. Marschall, D. Hui, B. Adair, and M. Vestel, *J. Am. Ceram. Soc.* **91**, 1481 (2008).
- [3] R. B. Kaner, J. J. Gilman, and S. H. Tolbert, *Science* **308**, 1268 (2005).
- [4] X. Blase, P. Gillet, A. San Miguel, and P. Mélinon, *Phys. Rev. Lett.* **92**, 215505 (2004).
- [5] A. Merlen, P. Toulemonde, S. Le Floch, G. Montagnac, T. Hammouda, O. Marty, and A. San Miguel, *Carbon* **47**, 1643 (2009).
- [6] H. O. Pierson, *Handbook of Refractory Carbides and Nitrides* (Noyes Publication, Westwood, New Jersey, USA, 1996).
- [7] A. F. Young, C. Sanloup, E. Gregoryanz, S. Scandolo, R. J. Hemley, and H.-k. Mao, *Phys. Rev. Lett.* **96**, 155501 (2006).
- [8] J. C. Crowhurst, A. F. Goncharov, B. Sadigh, C. L. Evans, P. G. Morrall, J. L. Ferreira, and A. J. Nelson, *Science* **311**, 1275 (2006).
- [9] E. Gregoryanz, C. Sanloup, M. Somayazulu, J. Badro, G. Fiquet, H.-k. Mao, and R. J. Hemley, *Nature Mater.* **3**, 294 (2004).
- [10] E. A. Juarez-Arellano, B. Winkler, A. Friedrich, D. J. Wilson, M. Koch-Müller, K. Knorr, S. C. Vogel, J. J. Wall, H. Reiche, W. Crichton, M. Ortega-Aviles, and M. Avalos-Borja, *Z. Kristallogr.* **223**, 492 (2008).
- [11] S. Ono, T. Kikegawa, and Y. Ohishi, *Solid State Commun.* **133**, 55 (2005).
- [12] H. Hahn and A. Konrad, *Z. Anorg. Allg. Chem.* **264**, 174 (1951).
- [13] P. Clark, B. Dhandapani, and S. T. Oyama, *Appl. Catal., A* **184**, L175 (1999).
- [14] R. Kojima and K.-i. Aika, *Appl. Catal., A* **209**, 317 (2001).
- [15] A. ul. Haq and O. Meyer, *J. Low Temp. Phys.* **50**, 123 (1983).
- [16] G. Soto, A. Rosas, M. H. Farias, W. De la Cruz, and J. A. Diaz, *Mater. Charact.* **58**, 519 (2007).
- [17] M. Fuchigami, K. Inumaru, and S. Yamanaka, *J. Alloys Compd.* **486**, 621 (2009).
- [18] H. K. Mao, J. Xu, and P. M. Bell, *J. Geophys. Res.* **91**, 4673 (1986).
- [19] W. A. Caldwell, M. Kunz, R. S. Celestre, E. E. Domning, M. J. Walter, D. Walker, J. Glossinger, A. A. MacDowell, H. A. Padmore, R. Jeanloz, and S. M. Clark, *Nucl. Instrum. Methods Phys. Res., Sect. A* **582**, 221 (2007).
- [20] A. P. Hammersley, S. O. Svensson, M. Hanfland, A. N. Fitch, and D. Hausermann, *High Press. Res.* **14**, 235 (1996).
- [21] K. Syassen, “Datlab, version 1.38XP,” MPI/FKF Stuttgart, Germany (2005).
- [22] L. J. Farrugia, *J. Appl. Crystallogr.* **32**, 837 (1999).
- [23] P.-E. Werner, L. Eriksson, and M. Westdahl, *J. Appl. Crystallogr.* **18**, 367 (1985).
- [24] A. C. Larson and R. B. Von Dreele, GSAS, Tech. Rep. Los Alamos National Laboratory Report LAUR, 1994.
- [25] M. Kunz, N. Tamura, K. Chen, A. A. MacDowell, R. S. Celestre, M. M. Church, S. Fakra, E. E. Domning, J. M. Glossinger, J. L. Kirschman, G. Y. Morrison, D. W. Plate, B. V. Smith, T. Warwick, V. V. Yashchuk, H. A. Padmore, and E. Ustundag, *Rev. Sci. Instrum.* **80**, 035108 (2009).
- [26] N. Tamura, A. A. MacDowell, R. Spolenak, B. C. Valek, J. C. Bravman, W. L. Brown, R. S. Celestre, H. A. Padmore, B. W. Batterman, and J. R. Patel, *J. Synchrotron Radiat.* **10**, 137 (2003).
- [27] S. J. Clark, M. D. Segall, C. J. Pickard, P. J. Hasnip, M. I. J. Probert, K. Refson, and M. C. Payne, *Z. Kristallogr.* **220**, 567 (2005).
- [28] Z. Wu and R. E. Cohen, *Phys. Rev. B* **73**, 235116 (2006).
- [29] H. J. Monkhorst and J. D. Pack, *Phys. Rev. B* **13**, 5188 (1976).
- [30] E. A. Juarez-Arellano, B. Winkler, A. Friedrich, L. Bayarjargal, V. Milman, J. Yan, and S. M. Clark, *J. Alloys Compd.* **481**, 577 (2009).